Correction: ΔNp63 Versatilely Regulates a Broad NF-κB Gene Program and Promotes Squamous Epithelial Proliferation, Migration, and Inflammation

Next Section

In this article (Cancer Res 2011;71:3688–700), which was published in the May 15, 2011, issue of Cancer Research (1), the graph in Fig. 7D was mislabeled because of a production error. The corrected figure appears below.

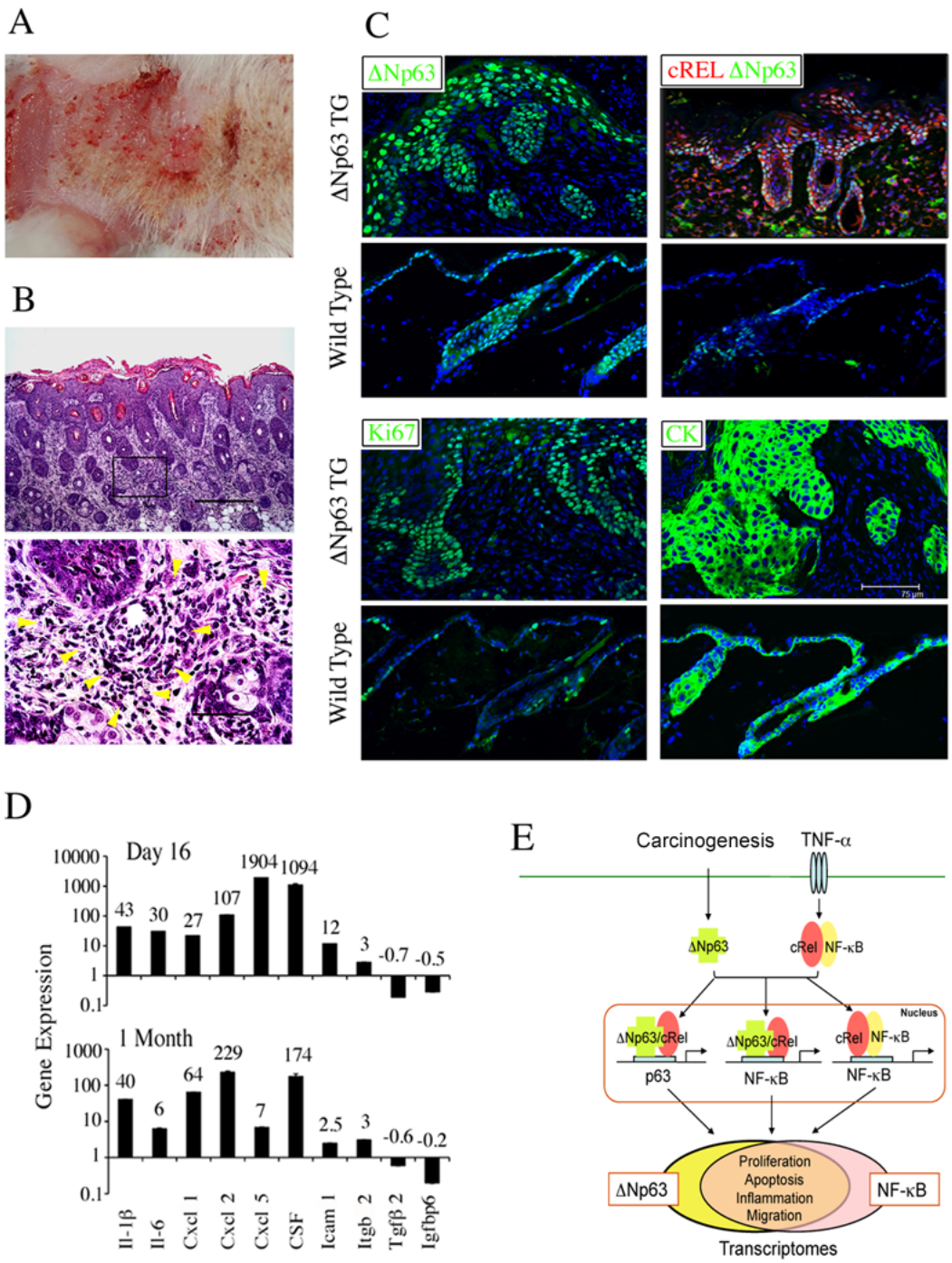
A
B
C
ΔNp63
cREL ΔNp63
ΔNp63 TG
Wild Type
Ki67
CK
75μm
D
Day 16
1 Month
Gene Expression
10000
1000
100
10
1
0.1
43
30
27
107
1904
1094
12
3
-0.7
-0.5
40
6
64
229
7
174
2.5
3
-0.6
-0.2
Il-1β
Il-6
Cxcl 1
Cxcl 2
Cxcl 5
CSF
Icam 1
Itgb 2
Tgfβ 2
Igfbp6
E
Carcinogenesis
TNF-α
ΔNp63
cRel
NF-κB
Nucleus
ΔNp63/cRel
p63
NF-κB
Proliferation
Apoptosis
Inflammation
Migration
Transcriptomes

Figure 7

2/1/2011

Supplementary information

ΔNp63 versatilely regulates a broad NF-κB gene program and promotes squamous epithelial proliferation, migration and inflammation

Xinping Yang,[1] Hai Lu, [1] Bin Yan, [1] Rose-Anne Romano,[2] Yansong Bian, [1] Jay Friedman,[1] Praveen Duggal,[1] Clint Allen,[3] Ryan Chuang,[1] Reza Ehsanian, [1,4,5] Han Si, [1] Satrajit Sinha,[2] Carter Van Waes,[1,6] and Zhong Chen[1,6]

Supplementary Experimental Procedures

UM-SCC Cell Lines. A panel of nine HNSCC cell lines from the University of Michigan squamous cell carcinoma (UM-SCC) series was obtained from Dr. TE Carey (University of Michigan, Ann Arbor, MI). These UM-SCC cell lines tested negative for HPV, and were extensively characterized in our previous studies, where they were found to reflect molecular and phenotypic alterations important in pathogenicity of HNSCC (9, 10). TP53 mutation status of these cell lines was analyzed by bi-directional DNA sequencing of exons 1-9 (10, 11). HNSCC cell lines used in this study are represented from the different sites of upperaerodigestive track: UM-SCC 6 (tongue), UM-SCC 1 (floor of mouth), UM-SCC 22B (lymph node metastasis from hypopharynx), UM-SCC 38 (tonsil/base of tongue), UM-SCC 46 (larynx). Primary human epidermal keratinocytes (HEKA) were purchased and cultured as previously described (Invitrogen), and cells were used within five passages. Subsequent microarray profiling studies have confirmed that HEKA and human oral

mucosa keratinocytes (HOK) exhibit similar expression patterns for ΔNp63 and other genes presented in this study (data not shown).

Reagents. The expression plasmids for ΔNp63α and TAp63α were kindly provided by Drs. James W Rocco and Leif W. Ellisen (Massachusetts General Hospital and Harvard University, Boston, MA) (1). Murine keratinocytes adenovirally infected with ΔNp63α, TAp63α, and ΔNp63γ expression vectors, were kindly provided by Dr. Weinberg (FDA, Bethesda, MD). The plasmid containing 5XNF-kB consensus binding sites with luciferase reporter gene was purchased from Stratagene (La Jolla, CA). TP53 reporter vector containing the firefly luciferase reporter gene was obtained from Panomics, Inc (Redwood City, CA). The luciferase plasmids containing IL-8 promoter sequence (-1481~+44bp from TSS) with serial deletions or point mutations were kindly provided by Dr. Naofumi Mukaida (2). The longest promoter construct contains a predicted p63 (-1435bp ~ -1406bp), AP-1 (-635bp ~ -625bp) (Yan L, manuscript in preparation). Other binding sites, such as AP-1 (-126bp ~ -120bp), NF-IL6 (-94bp ~ -81bp) and p65/cRel (-83bp ~ -71bp) are previously described (2, 3). The luciferase plasmid containing ~2.6kb p21 promoter sequence was from Dr. Vogelstein's laboratory (4). TNF-α was purchased from R&D Systems (Minneapolis, MN), and Qunacrine was purchased from Calbiochem, (Gibbstown, NJ). The sequence of p63 siRNA targeting the unique exon in the N-terminal of ΔNp63 was according to previous publication (5), and the siRNA targeting ΔNp63 was made by Integrated DNA Technologies (IDT, Coralville, IA). All other siRNAs were purchased from Dharmacon through ON-TARGETplus of SMART selection (Chicago, IL). A control siRNA was purchased from Qiagen (Valencia, CA). WST-1 cell proliferation reagent was purchased from Roche (Indianapolis, IN).

Antibodies. IHC and Western blot: goat anti-ΔN-p63 (Santa Cruz, N-16), mouse anti-TP53 (Calbiochem, DO-1), mouse anti-pan cytokeratin (Novocastra), mouse anti-Ki67 (Dako, MIB-1), anti-β4 integrin (Ancell, UMA9), mouse anti-p63, (Santa Cruz, 4A4); rabbit anti-β-actin (Cell Signaling). ChIP and EMSA: rabbit anti-p63 (Santa Cruz, H-129 and H137), rabbit anti-cRel (Santa Cruz, sc-71x), rabbit anti-cRel (Millipore, 09-040), mouse anti-IKK〈 (IMGENEX, IMG-136A), rabbit anti-RelA (Upstate, 06-418, ChIP), rabbit anti-RelA (Santa Cruz, sc-109x, EMSA), normal mouse (Upstate, 12-371B), or rabbit IgG (Upstate, Santa Cruz). Immunofluorescent staining of ΔNp63α TG mice: anti-ΔNp63 (RR-14), anti-Ki67 (Novocastra), and anti-K14 (1:200, gift from Dr Julie Segre) (6).

IHC analysis of frozen HNSCC tissue specimens. Frozen tissue samples of HNSCC were obtained from the Cooperative Human Tissue Network (CHTN) and sectioned. Detailed procedure for immunohistochemistry (IHC) and the histoscore were described previously (7, 8), which combine both staining intensity and percentage cells stained. The primary antibodies used for immunostaining were as follows: goat anti-ΔN-p63 (N-16, Santa Cruz Biotechnology), mouse anti-human TP53 (DO-1, Calbiochem), mouse anti-human pan cytokeratin (Novocastra), mouse anti-Ki67 (Dako, MIB-1), and anti-β4 integrin (Ancell, UMA9). The histology images were taken under microscope at 400X magnification. The classification of tumor samples was based on the staining intensity. Based on ΔNp63 histoscore, 18 tumor specimens exhibit intermediate or strong ΔNp63 staining, and the remaining 6 tumor samples show weak or no ΔNp63 staining.

Tissue Array and IHC. Formalin-fixed and paraffin-embedded HNSCC tissue arrays were obtained from Cybrdi (Rockville, MD) and previously described (10). Each array contained HNSCC tumor tissues from 20 individuals spotted in triplicate, plus normal mucosa tissues from 6 normal subjects spotted in duplicate. Briefly, the tissue slides were dewaxed in xylene, hydrated through graded alcohols, and incubated in 3% hydrogen peroxide in PBS for 30 min to block the endogenous peroxidase. After washing in distilled water, antigen retrieval was performed with 10 mM citric acid in a microwave for 20 min. Slides were allowed to cool down to room temperature, rinsed thoroughly with distilled water and PBS, then incubated in blocking solution (2.5% BSA in PBS) for 30 min at room temperature. Then sections were incubated overnight at 4 °C with the primary antibody diluted in blocking solution. The primary antibodies included anti-ΔNp63 (1:100, N16, Santa Cruz, Santa Cruz, California); mouse anti-Ki-67 (1:100, TEC-3, DAKO, Carpinteria, CA). The slides were sequentially incubated with the biotinylated secondary antibody (1:400; Vector, Burlingame, CA) for 30 min, followed by the avidin-biotin complex method (Vector Stain Elite, PK-6100 Standard ABC kit; Vector, Burlingame, CA) for 30 min at room temperature. The slides were washed and developed in 3'3'-diaminobenzidine (FASTDAB tablet; Sigma, St. Louis, MO). The reaction was stopped in tap water, and the tissues were counterstained with hematoxylin, dehydrated, and mounted. Whole slide images were acquired using an Aperio Scanscope at X20 magnification. Relevant areas were quantified as histological score which is calculated by multiplying the intensity score (0-3) by the percentage of positive cells (0-100) showing in that intensity, using the Aperio Cell Quantification Software (Aperio, Vista, CA). An outlier was excluded by Cook's distance

$\geq$ 0.8. The coefficiency of IHC intensity of ΔNp63 and Ki67 expression was calculated by Pearson Correlation, and the statistical significance was presented by p value.

Real time RT-PCR. RNA isolation and cDNA synthesis were performed as previously described (10). Real time PCR primers and probes for human and mouse ΔNp63 and TAp63 were synthesized by Applied Biosystems (Foster City, CA), according to previous publications (12, 13). Other primers and probes were purchased through Assays-on-Demand™ program from Applied Biosystems. Amplification conditions were: 2 min at 50^{o}C and 10 min at 95^{o}C, followed by 40 cycles of 15 sec at 95^{o}C and 1 min at 60^{o}C, carried out using an ABI Prism 7700 Sequence Detection System (Applied Biosystems). Relative gene expression values were calculated after normalization to 18S rRNA. Each experiment was done in duplicates, and each sample was assayed in triplicates. Data were presented as mean $\pm$ standard deviation (SD).

Western blotting analysis. Whole cell lysates were obtained using a Nuclear Extraction Kit from Active Motif according to the manufacturer's protocol (Carlsbad, CA). Western blot analysis was performed using Tris-Glycine or Bis-Tris pre-cast gels (Invitrogen) as previously described (11). Primary antibodies were used: mouse monoclonal anti-TP53, 1:1000 (clone DO-1, Calbiochem); mouse monoclonal anti-p63, 1:500 (4A4, Santa Cruz); rabbit polyclonal anti-β-actin, 1:2000, (Cell Signaling Technology). Signals were detected using horseradish peroxidase linked anti-mouse or anti-rabbit (1:4000) secondary antibody (Chemicon). Each blot was incubated with Pierce Super Signal West Pico substrate (Pierce Biotechnology Inc) and exposed to Kodak X-OMAT film.

Reporter gene assays. UM-SCC cell culture, transfection, and cellular lysate isolation were performed as previously described (14). Reporter gene activities were assayed using Dual-Light System kit (Applied Biosystems), and measured by Wallac VICTOR2 1420 Multilabel Counter (Perkin Elmer). The reporter gene activities were adjusted to β-gal activities or WST1 based cell proliferation assay (Roche Diagnostics). Each experiment was performed in triplicates, and each sample was assayed in duplicates. Data were presented as mean $\pm$ SD.

Analysis of networks and pathways. The genes identified as ΔNp63 targets were imported into IPA 5.0 (Ingenuity Systems Inc, Mountain View, CA) according to the Ingenuity Pathways Knowledge Base (IPKB), where each interaction in IPKB is supported by the underlying publications and structured functional annotation. Statistical scores were then assigned to rank the resulting networks and pathways using Fisher's right tailed exact test, where significant networks ($P<0.001$) and pathways ($P<0.05$) were selected. IPA allows comparison of gene networks and pathways generated by different sets of input genes, or under the regulations of different transcription factors. In this study, we input RELA or NFκB1 to the ΔNp63 target gene network to identify RELA or NFκB1 direct interaction and networks. The gene cluster and heatmap was illustrated using Cluster 2.11 and Java TreeView software developed by Eisen's laboratory (UC Berkeley, Berkeley, CA). The predicted transcription binding sites inside -500bp to +100bp of the promoter regions from the transcription starting sites were generated using Genomatix software (Munchen, Germany).

Chromatin Immunoprecipitation Assay (ChIP). ChIP assays were performed using the EZ ChIP Assay Kit (Upstate Biotechnology). Briefly, precleared chromatin was immunoprecipitated with 2μg rabbit IgG against p63 (H-129, Santa Cruz), rabbit IgG against cRel (sc-71x, Santa Cruz), mouse monoclonal IgG1 against IKKα (IMG-136A, IMGENEX), rabbit IgG against p65 (06-418, Upstate), normal mouse IgG (12-371B, Upstate), or rabbit IgG (Upstate). Precipitated DNA was amplified using Power SYBR Green PCR Master Mix (Applied Biosystems) and quantified for 50 cycles by an ABI Prism 7700 Sequence Detection System (Applied Biosystems). The specificity of PCR products was assured by running a 2% agarose E-Gel (Invitrogen). Primers were designed using the OligoPerfect Designer (Invitrogen), base on predicted binding motifs. The primer sequences are presented in Supplemental Table S4.

Predicted p63 and NF-κB p65/cREL binding sites and designed PCR primers used in ChIP assay. The putative p63 binding sites on ΔNp63 target gene promoters were predicted based on position weighted matrixes (PWM) built according to several publications and databases (Bin Yan et al, manuscript in preparation). We selected 28 top scored putative p63 and 2 cRel binding sites in the range of -3000bp to +1000bp from the transcription stating site (TSS) of promoters. An initial screen by ChIP identified significant basal levels of p63 binding activities on 13 sites of 8 gene promoters, including a known p63 binding site in the p21 gene (Supplementary Table S4) (15, 16). The sequences of these binding sites and designed primers are as follows: CSF2, p63 binding site (+845bp): GGGCAGGTTCGTGCCTGCCAT; forward primer: 5'-GGGGTGAGAGTCACCTCCTT-3'; reverse primer: 5'-GTCATAGACCCTGCCCTGTC-3'; amplicon: 122bp (+764~+885). PDGFA, p63 binding site (-1495bp):

ACCACCCAGAGGGCATGCTTG; forward primer: 5'-AAGGCTCCCCTGGTTCTGT-3'; reverse primer: 5'-ACGTCTCTCCCTTCCGTTG-3'; amplicon: 109bp (-1426~-1535). IL8, p63 binding site (-1424bp): TAACAAAAAGAAACATGATTG; forward primer: 5'-CCCAGGCATTATTTTATCCTCA-3'; reverse primer: 5'-GCCATTTTCAAATGCTTTCC-3'; amplicon: 110bp (-1361~-1470). IL8, p65/cREL binding site (-83bp): CGTGGAATTTCCT; forward primer: 5'-CATCAGTTGCAAATCGTGGA-3'; reverse primer: 5'-GTTTGTGCCTTATGGAGTGCT-3'; amplicon: 110bp (-108~+6). YAP1 p63 binding site (-2324bp), forward primer: 5'-CTGGAGTGCAGTGGTGTGAT-3'; reverse primer: 5'-GTGGTGGCATGTTCCTGTAGT-3', amplicon: 115bp; and the cREL site (-2218bp), forward primer: 5'-CCACCACACCTGGCTAATTT-3', reverse primer: 5'-CTGTAG

TCCCAGCACTTTGG-3', amplicon: 135bp. Additional information of other primers are shown in Supplementary Table S4.

Chromatin Immunoprecipitation Assay (ChIP)

Protein-DNA complexes were precipitated by rabbit anti-p63 (H-129, Santa Cruz), rabbit anti-cRel (sc-71x, Santa Cruz), mouse anti-IKKα (IMG-136A, IMGENEX), rabbit anti-p65 (06-418, Upstate), and normal IgG controls (Upstate) using EZ ChIP Assay Kit (Upstate). Briefly, precipitated DNA was amplified using SYBR Green PCR Master Mix (Applied Biosystems) by an ABI Prism 7700 Sequence Detector (Applied Biosystems). Primers were designed using the OligoPerfect Designer (Invitrogen, Supplementary Table S4).

Electrophoretic mobility shift assay (EMSA). The oligonucleotides for EMSA covering IL-8 promoter p65/cRel binding site (-83bp) was [γ-^{32}P]-end-labeled with 10 U of T4 polynucleotide kinase (New England Biolabs) (3). EMSA was performed using LightShift Chemiluminescent Electrophoretic Mobility Shift Assay Kit (Pierce). The oligo probe of IL-8 promoter p65/cRel binding site (-83bp) is 5'-GATCGTGGAATTTCCTCTC-3' (17), the mutant oligo probe was mutated one base pair highlighted by underline, 5'-GATCGTG**C**AATTTCCTCTC-3'. The oligo probe of IL-8 promoter p63 site (-1424bp) is 5'-TAACAAAAAGAAACATGATTGTGCAGAAA

C-3', CSF2 promoter p63 binding site (+845bp) is 5'-GGCAGTGAGAAGGGCAGGTTCGTGCCTGCCATGGACAGGGCA-3', and the probe for cREL site (+702) of CSF promoter is 5'-GGTTTCAGGAACAACCCTTGCCCAC-3', and p63 site (-2324bp) of YAP promoter is 5'-GGGACTACAGGAACATGCCACCACACCTGG-3' based on our prediction. The supershift used anti-p65 (sc-109x), anti-p63α (H129 and H137), and anti-cRel antibodies (Santa Cruz and Millipore). Nuclear extracts (5 μg/reaction) were incubated at room temperature with 1 μl of labeled probe (20,000 cpm) and resolved by 4% polyacrylamide gel, followed by autoradiography. For a negative control, unlabeled oligonucleotide was added in 200-fold excess.

MTT cell proliferation assay. UM-SCC cells were initially plated in 6 well plates and transfected with siRNA targeting ΔNp63. The following day cells were trypsinzed and harvested, counted and replated into 96 well plates at 5 x 10^3 cells per well in 100 μl of complete medium in quadruplicates. Cell proliferation was measured using a 3-(4,5-

dimethylthiazol-2-yl)-2,5-diphenyltetrazolium bromide (MTT) Cell Proliferation Kit (Roche Diagnostics, Indianapolis, IN). The optical density was measured by a μQuant microplate reader (Bio-Tek Instrument, Winooski, VT) at a wavelength of 570 nm.

DNA based cell cycle and apoptotic flow analysis. UM-SCC 1 cells were plated in 6 well plates and transfected under conditions previously stated (18). At 48, 72 or 96 hours, cells were trypsinized, counted and labeled using the Cycletest Plus DNA regent kit (BD Biosciences, San Jose, CA) following the standard protocol. Samples were run on FACS Canto machine within 1 hour and analyzed using DIVA flow cytometric analysis software.

Wound healing and Matrigel migration assays. Cells were transfected with siRNA for 24 hours. Wounds were made through the confluent cell sheets using a 1ml pipette tip. Scratches were monitored for % wound closure over the next 48 hours. Twelve measurements at preset distances on the wound were measured and quantified. The statistical analysis relative to the control siRNA was performed (t-test, * $p<0.05$). To further confirm the effect of knocking down ΔNp63 on cell migration, Matrigel migration assay was performed using BD Biocoat Growth Factor Reduced Matrigel Invasion Chamber (Cat# 354483, BD Bioscience). Briefly, cells were transfected with siRNA for 48 hours using the culture and transfection conditions as described in this study. Then the cells were detached from the culture dishes by treating with 1X accutase according to manufacturer's protocol (Sigma, Cat#A6964). The cells were counted and plated at $5X10^4$ cells/insert well of Matrigel plate in duplicates using DMEM serum free medium for 24 hours. The bottom well was plated with DMEM serum free medium plus 10ng/ml

EGF (R&D Systems). The membranes with migrated cells were harvested, stained with crystal violet, and mounted onto the glass slides. The cell images were scanned and analyzed by ScanScope Aperio Digital Pathology System (Aperio Technologies, Inc, Vista, CA). The quantitation of migrated cells was performed by cell counts of 4 representative 40X fields of duplicated wells and presented as mean $\pm$ standard deviation (SD). The statistical significance was tested by Student t test, and * indicates $p<0.05$.

Generation of conditional ΔNp63α transgenic mouse model. The generation of the Tet-responsive ΔNp63α transgenic mouse model has been described (6, 19). Briefly, the HA-ΔNp63α construct was generated by cloning the full-length mouse ΔNp63α containing a 5' HA epitope tag into the pTRE Tight plasmid (BD Bioscience). Transgenic mouse lines were generated by microinjecting the purified DNA constructs into fertilized mouse oocytes. Seven HA-ΔNp63α transgenic founder lines were identified by PCR analysis of tail DNA. In order to determine which of the seven transgenic founder animals inducibly express ΔNp63α, we crossed each of the founders to the previously characterized tet-OFF transgenic mice expressing the tetracycline transactivator (tTA) under the control of the bovine K5 promoter (K5-tTA), which is active in the basal keratinocytes of the skin (6). Four founding lines (B, D, E and F) were identified to express the transgene by Western blot analysis and they exhibited varying levels of phenotypic severities in the skin. Expression of ΔNp63α in the bitransgenic animals (K5-tTA/pTRE-ΔNp63α or ΔNp63α BG) was induced after birth by feeding the pregnant dams with chow supplemented with Dox.

After ΔNp63α was specifically induced, the ΔNp63α TG mice began to develop skin lesions and erythema within one month. The areas affected by lesions were primarily in the back and flank regions and to a large extent overlapped with the regions of mouse grooming. The scaling and desquamation of the skin and wounding scabs, particularly in the axillary areas susceptible to frictional trauma, progressed with time such that the lesions became rapidly larger, eventually destroying the skin surfaces and causing irrepairable damage and animals had to be euthanized in 3-4 months after induction to minimize suffering. Upon histological analysis of the affected areas, the epidermis of the ΔNp63α TG animals appeared hyperplastic (acanthosis) and hyperproliferative with signs of, hyperkeratosis, hypogranulosis, and parakeratosis and clear evidence of infiltrating cells in the dermis (Fig. 7A and B). In contrast, skin from wild type or ΔNp63αTG mice, where expression of transgene was suppressed by Dox treatment, displayed typical features of a thin epidermis with normal hair follicles (data notshown).

Immunofluorescence. Paraffin embedded dorsal skin sections were sectioned to 4μm thickness. Slides were de-paraffinized and rehydrated, and antigen retrieval was performed by boiling slides in a microwave for 20 minutes in 10mM sodium citrate solution (0.05% Tween-20, pH 6.0). Slides were blocked in 5% BSA, 0.1% TritonX-100 in PBS for 1 hour. The primary antibodies used were K14, ΔNp63 (RR-14) (1:50), and Ki67 (1:50; Novocastra) (6). Slides were mounted using Vectashield Mounting Medium with DAPI (Vector Labs) and viewed under a Nikon FXA fluorescence microscope. Images were captured using a Nikon digital camera and analyzed using ImageJ, Adobe Photoshop, and Adobe Illustrator software.

Supplementary References:

1. Rocco JW, Leong CO, Kuperwasser N, DeYoung MP, Ellisen LW. p63 mediates survival in squamous cell carcinoma by suppression of p73-dependent apoptosis. Cancer Cell 2006; 9: 45-56.
2. Mori N, Mukaida N, Ballard DW, Matsushima K, Yamamoto N. Human T-cell leukemia virus type I Tax transactivates human interleukin 8 gene through acting concurrently on AP-1 and nuclear factor-kappaB-like sites. Cancer Res 1998; 58: 3993-4000.
3. Ondrey FG, Dong G, Sunwoo J, et al. Constitutive activation of transcription factors NF-(kappa)B, AP-1, and NF-IL6 in human head and neck squamous cell carcinoma cell lines that express pro-inflammatory and pro-angiogenic cytokines. Mol Carcinog 1999; 26: 119-29.
4. el-Deiry WS, Tokino T, Velculescu VE, et al. WAF1, a potential mediator of p53 tumor suppression. Cell 1993; 75: 817-25.
5. Thurfjell N, Coates PJ, Vojtesek B, Benham-Motlagh P, Eisold M, Nylander K. Endogenous p63 acts as a survival factor for tumour cells of SCCHN origin. Int J Mol Med 2005; 16: 1065-70.
6. Romano RA, Ortt K, Birkaya B, Smalley K, Sinha S. An active role of the DeltaN isoform of p63 in regulating basal keratin genes K5 and K14 and directing epidermal cell fate. PLoS One 2009; 4: e5623.
7. Van Waes C, Chang AA, Lebowitz PF, et al. Inhibition of nuclear factor-kappaB and target genes during combined therapy with proteasome inhibitor bortezomib and reirradiation in patients with recurrent head-and-neck squamous cell carcinoma. Int J Radiat Oncol Biol Phys 2005; 63: 1400-12.
8. Nenutil R, Smardova J, Pavlova S, et al. Discriminating functional and non-functional p53 in human tumours by p53 and MDM2 immunohistochemistry. J Pathol 2005; 207: 251-9.
9. Yan B, Yang X, Lee TL, et al. Genome-wide identification of novel expression signatures reveal distinct patterns and prevalence of binding motifs for p53, nuclear factor-kappaB and other signal transcription factors in head and neck squamous cell carcinoma. Genome Biol 2007; 8: R78.
10. Lee TL, Yang XP, Yan B, et al. A Novel Nuclear Factor-{kappa}B Gene Signature Is Differentially Expressed in Head and Neck Squamous Cell Carcinomas in Association with TP53 Status. Clin Cancer Res 2007; 13: 5680-91.
11. Friedman J, Nottingham L, Duggal P, et al. Deficient TP53 Expression, Function, and Cisplatin Sensitivity Are Restored by Quinacrine in Head and Neck Cancer. Clin Cancer Res 2007; 13: 6568-78.
12. Signoretti S, Waltregny D, Dilks J, et al. p63 is a prostate basal cell marker and is required for prostate development. Am J Pathol 2000; 157: 1769-75.
13. Koster MI, Dai D, Marinari B, et al. p63 induces key target genes required for epidermal morphogenesis. Proc Natl Acad Sci U S A 2007; 104: 3255-60.

14. Worden B, Yang XP, Lee TL, et al. Hepatocyte growth factor/scatter factor differentially regulates expression of proangiogenic factors through Egr-1 in head and neck squamous cell carcinoma. Cancer Res 2005; 65: 7071-80.
15. Westfall MD, Mays DJ, Sniezek JC, Pietenpol JA. The Delta Np63 alpha phosphoprotein binds the p21 and 14-3-3 sigma promoters in vivo and has transcriptional repressor activity that is reduced by Hay-Wells syndrome-derived mutations. Mol Cell Biol 2003; 23: 2264-76.
16. King KE, Ponnamperuma RM, Allen C, et al. The p53 homologue DeltaNp63alpha interacts with the nuclear factor-kappaB pathway to modulate epithelial cell growth. Cancer Res 2008; 68: 5122-31.
17. Mitsuyama H, Kambe F, Murakami R, Cao X, Ishiguro N, Seo H. Calcium signaling pathway involving calcineurin regulates interleukin-8 gene expression through activation of NF-kappaB in human osteoblast-like cells. J Bone Miner Res 2004; 19: 671-9.
18. Lee TL, Yeh J, Friedman J, et al. A signal network involving coactivated NF-kappaB and STAT3 and altered p53 modulates BAX/BCL-XL expression and promotes cell survival of head and neck squamous cell carcinomas. Int J Cancer 2008; 122: 1987-98.
19. Romano RA, Smalley K, Liu S, Sinha S. Abnormal hair follicle development and altered cell fate of follicular keratinocytes in transgenic mice expressing DeltaNp63alpha. Development 2010; 137: 1431-9.

Supplementary Figure Legends:

Figure S1. ΔNp63 overexpression in HNSCC tissues and cell lines. A, frozen sections of mucosa (left) and 21 HNSCC specimens stained with antibodies against ΔNp63 (N-16) and pan cytokeratin (pan CK), and counterstained with hematoxylin (400X magnification). Representative HNSCC samples are shown with none/weak, intermediate, or strong ΔNp63 staining intensity. B, left: ΔNp63 and TAp63 mRNA levels of normal HEKA and nine UM-SCC cell lines were quantified by real time RT-PCR, and presented after setting TAp63 expression in HEKA as 1 using log scale. Right: total p63 protein was detected by antibody (4A4) in whole cell lysates with controls expressing human TAp63α, ΔNp63α, TAp63γ proteins (M: molecular mass markers). β-actin was used as the loading control.

Figure S2. Knockdown efficiencies of ΔNp63, TAp63 and TP53, and ΔNp63 target genes in HNSCC cell lines. A, UM-SCC 1 cells were transiently transfected for 48 hours with siRNA targeting ΔNp63 (left), or with expression plasmids of ΔNp63 (second left), TAp63 (third left), or TP53 (right). No: no transfection; C: cells transfected with control siRNA, or control plasmids. Relative gene expression (fold changes compared with control siRNA) was quantified by real-time RT-PCR, and the statistical significance was presented (*, t test, $p<0.05$). Proteins were detected by Western blot using β-actin as the loading control. B, UM-SCC 1 cells were transfected with siRNA targeting ΔNp63, and mRNA was harvested at 24 (white bar), 48 (gray bar) and 72 (black bar) hrs post transfection. The relative gene expression was adjusted to control siRNA and presented as the fold changes (1.0 equals to 100% increased gene expression). The data are presented as (mean+SD) of PCR triplicates from duplicated samples. * indicates statistical significance (t test, $p<0.05$).

Figure S3. TNF-α, Quinacrine, ΔNp63 and TP53 regulate reporter activities. UM-SCC 1 cells were transiently transfected by siRNA targeting TP53 or ΔNp63 (second right column), or with TP53 expression vector (right column) for 48 hrs. TNF-α (1000U/ml for 48 hrs, left) and Quinacrine (QC, 5μM for 24 hrs, second left) were used as the positive controls for induction of NF-κB or p53 reporter activities, respectively. NF-κB, IL-8 promoter (-133bp), TP53 and p21 reporter activities were examined and adjusted with β-gal. * indicates statistical significance (t test, $p<0.05$). (-): no treatment, Ctrl: cells transfected with control siRNA, or control plasmids.

Figure S4. Knockdown of ΔNp63 inhibited cell proliferation, induced cell death, altered cell cycle, and decreased cell migration. A, UM-SCC 6 cells were transiently transfected with siRNA targeting ΔNp63, and cell proliferation was measured by MTT. * indicates statistical difference (t test, $p<0.05$). B, Cell cycle was measured at 48 hrs after transfection of ΔNp63 siRNA and DNA fragmentation (sub G0) was measured at 72hrs by flow cytometry in UM-SCC 1 cells in medium with 10% serum. Transfection conditions were shown as L: Lipofectamine alone. C: control siRNA; dN: ΔNp63 siRNA; TA: TAp63 siRNA. C. 24 hrs after ΔNp63 or TAp63 knockdown, monolayer of UM-SCC 1 cells was scratched, and the wound closure was measured at different time points and quantified from three areas from one representative of repeated experiments. * indicates significant difference (t test ($p<0.05$). D. Cell migration was measured by Matrigel assay and the representative images were presented at 100X magnification. The quantitation of migrated cells were performed by cell counts of multiple fields and presented as mean $\pm$ standard deviation (SD). The statistical significance was tested by Student t test, and * indicates $p<0.05$.

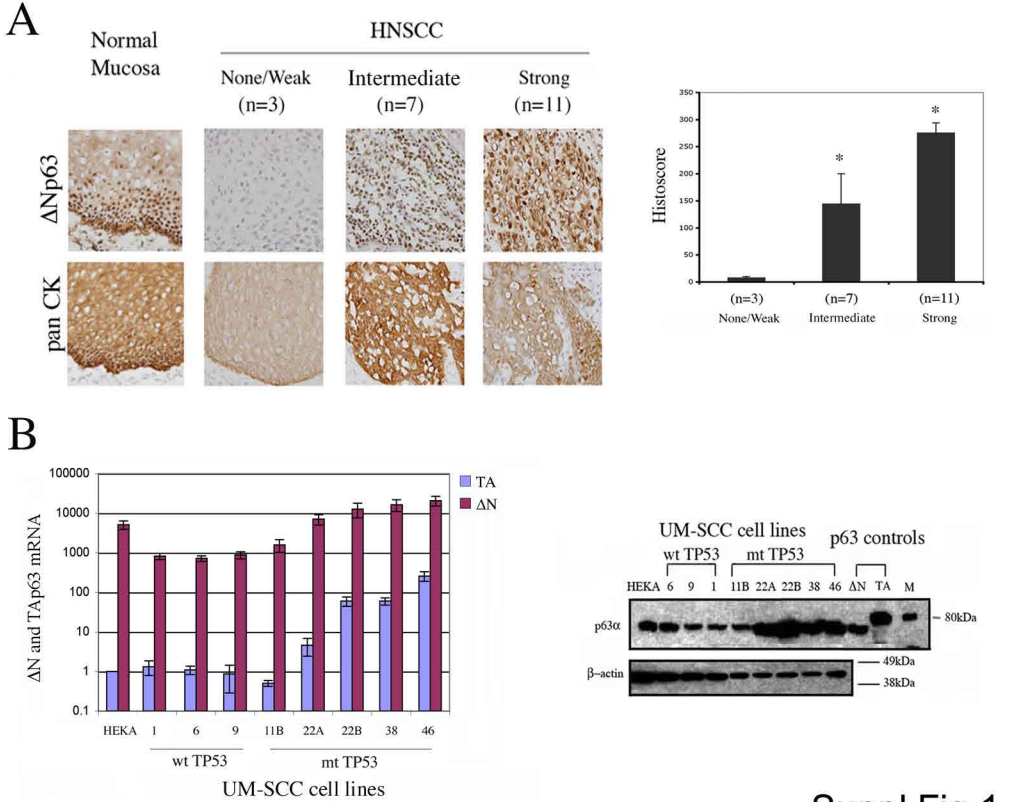
A
Normal Mucosa
HNSCC
None/Weak (n=3)
Intermediate (n=7)
Strong (n=11)
ΔNp63
pan CK
Histoscore
(n=3) None/Weak
(n=7) Intermediate
(n=11) Strong
B
ΔN and TAp63 mRNA
TA
ΔN
HEKA 1 6 9 11B 22A 22B 38 46
wt TP53
mt TP53
UM-SCC cell lines
UM-SCC cell lines
p63 controls
wt TP53
mt TP53
HEKA 6 9 1 11B 22A 22B 38 46 ΔN TA M
p63α
80kDa
β-actin
49kDa
38kDa

Suppl Fig 1

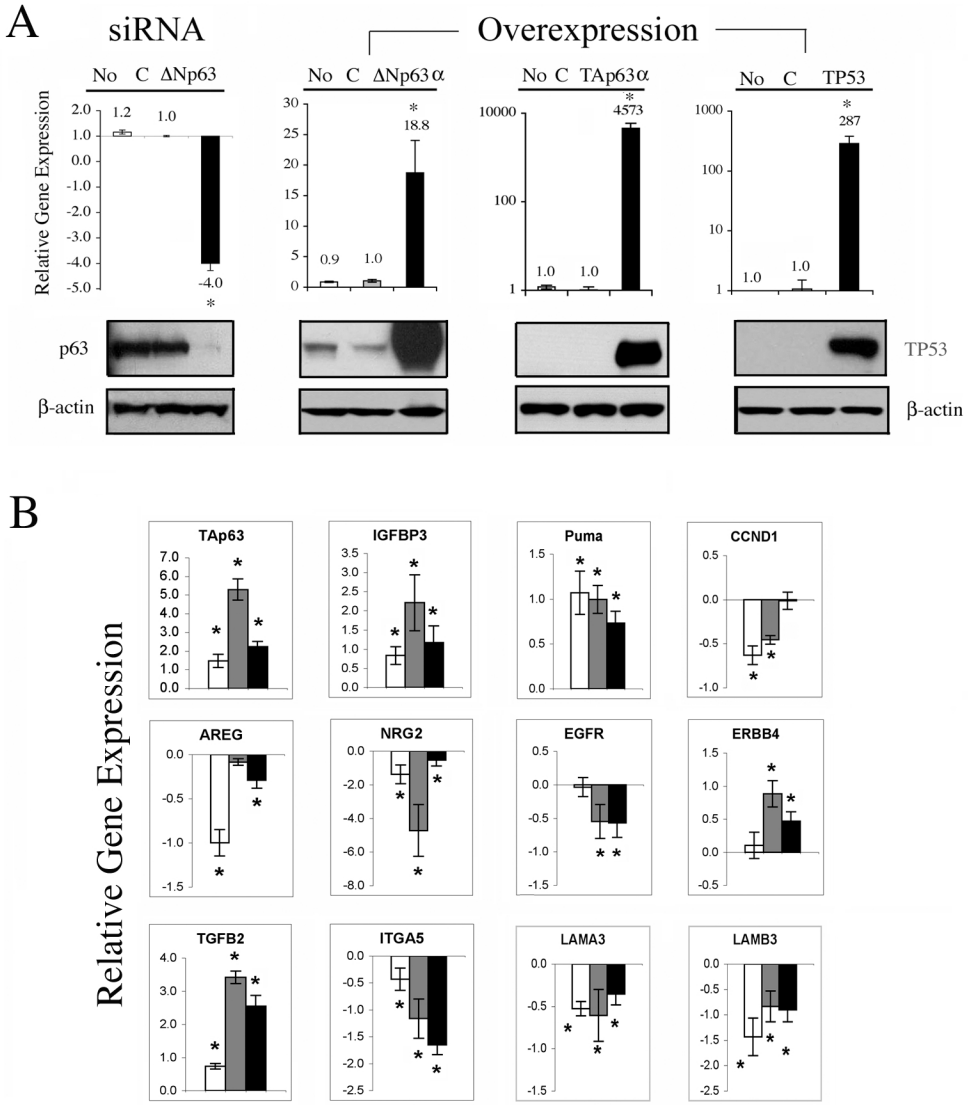
A
siRNA
Overexpression
No C ΔNp63
No C ΔNp63α
No C TAp63α
No C TP53
Relative Gene Expression
1.2
1.0
-4.0
0.9
1.0
18.8
1.0
1.0
4573
1.0
1.0
287
p63
β-actin
TP53
β-actin
B
Relative Gene Expression
TAp63
IGFBP3
Puma
CCND1
AREG
NRG2
EGFR
ERBB4
TGFB2
ITGA5
LAMA3
LAMB3

Suppl Fig 2

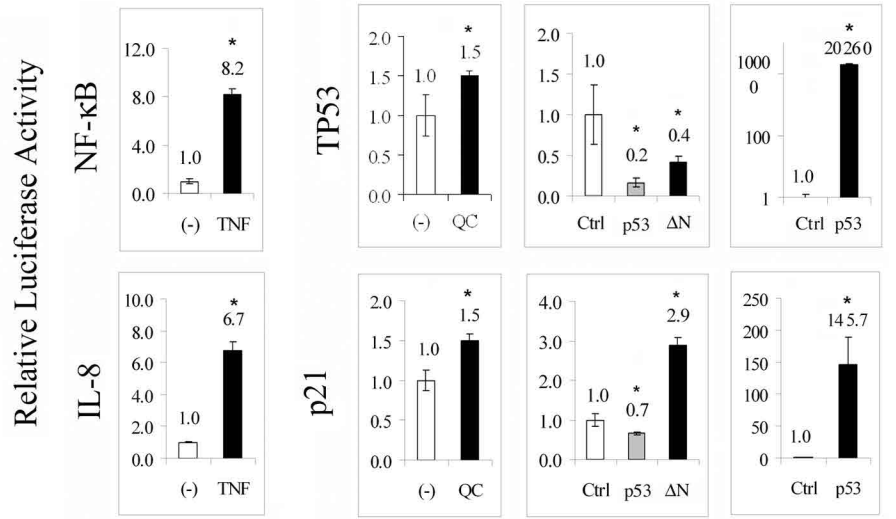
siRNA
Overexpression
Relative Luciferase Activity
NF-κB
IL-8
TP53
p21
12.0
8.0
4.0
0.0
1.0
8.2
(-)
TNF
10.0
6.7
2.0
2.0
1.5
1.0
QC
4.0
3.0
2.9
0.7
Ctrl
p53
ΔN
1000
100
1
20260
250
200
150
50
145.7

Suppl Fig 3

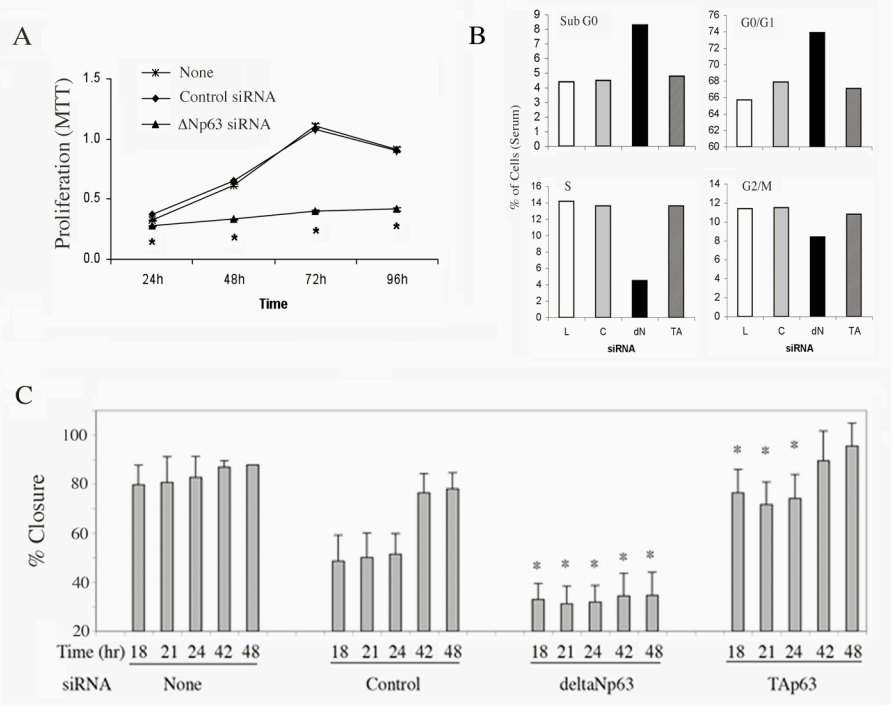

Supple Fig S4